J Mol Model (2006) 12: 390–397
DOI 10.1007/s00894-005-0058-y

ORIGINAL PAPER

Qiong Xie · Yun Tang · Wei Li · Xing-Hai Wang · Zhui-Bai Qiu

Investigation of the binding mode of (−)-meptazinol and bis-meptazinol derivatives on acetylcholinesterase using a molecular docking method

Received: 8 December 2004 / Accepted: 9 August 2005 / Published online: 11 January 2006

Abstract Molecular docking has been performed to investigate the binding mode of (−)-meptazinol (MEP) with acetylcholinesterase (AChE) and to screen bis-meptazinol (bis-MEP) derivatives for preferable synthetic candidates virtually. A reliable and practical docking method for investigation of AChE ligands was established by the comparison of two widely used docking programs, FlexX and GOLD. In our hands, we had more luck using GOLD than FlexX in reproducing the experimental poses of known ligands (RMSD<1.5 Å). GOLD fitness values of known ligands were also in good agreement with their activities. In the present GOLD docking protocol, (−)-MEP seemed to bind with the enzyme catalytic site in an open-gate conformation through strong hydrophobic interactions and a hydrogen bond. Virtual screening of a potential candidate compound library suggested that the most promising 15 bis-MEP derivatives on the list were mainly derived from (−)-MEP with conformations of (*S*,*S*) and (*SR*,*RS*) and with a 2- to 7-carbon linkage. Although there are still no biological results to confirm the predictive power of this method, the current study could provide an alternate tool for structural optimization of (−)-MEP as new AChE inhibitors.

Keywords Meptazinol (MEP) · Molecular docking · GOLD · Acetylcholinesterase (AChE)

Q. Xie · Y. Tang (✉) · W. Li · X.-H. Wang · Z.-B. Qiu (✉)
School of Pharmacy, Fudan University,
Shanghai, 200032, People's Republic of China
e-mail: ytang234@yahoo.com.cn
Tel.: +86-21-54237419
e-mail: zbqiu@shmu.edu.cn
Tel.: +86-21-54237595

Y. Tang (✉)
School of Pharmacy,
East China University of Science and Technology,
Shanghai, 200237, People's Republic of China
Tel.: +86-21-64251052

Introduction

Alzheimer's disease (AD) is a neurodegenerative disorder that seriously threatens the health of elderly people around the world. Although with an unclear pathogenesis, AD is commonly believed to be associated with the dysfunction of the central cholinergic system [1, 2]. Acetylcholinesterase (AChE) plays a key role in the regulation of the cholinergic system, and hence, inhibition of AChE has emerged as one of the most promising strategies for the treatment of AD. So far, four AChE inhibitors have been approved by the FDA in the US for treatment of AD, namely tacrine (THA) [3], donepezil (E2020) [4], rivastigmine [5] and galanthamine (GNT) [6]. In China (−)-Huperzine A (HUPA) [7] was also approved for the same purpose. Due to drawbacks such as hepatotoxicity and low selectivity as in the case of tacrine [8], the search for new AChE inhibitors with high selectivity and low toxicity remains an urgent task.

Meptazinol (MEP, Fig. 1) is a potent opioid analgesic but with less respiratory depression and low addiction liability [9], possibly due to a component of cholinergic activation presented in its pharmacological profile [10]. Early in 1986 Ennis et al. reported the inhibition of AChE by meptazinol [11], which not only confirmed MEP's involvement in the cholinergic system, but also opened a door in the search for new AChE inhibitors. Ennis' experiments demonstrated that (±)-MEP acted on AChE in vitro with an IC_{50} of 6.4 μM, while the (−)-enantiomer (IC_{50}=3.3 μM) was far more potent than its antipole (+)-enantiomer (IC_{50}>1.0 mM). The inhibitory potency of (−)-MEP was almost equivalent to that of (−)-galanthamine and tacrine, about 100 times less potent than physostigmine [11]. Recently, we determined the absolute configurations of (−) and (+)-MEP as S and R, respectively, by X-ray crystal structures (Fig. 1) [12]. Therefore, it was of considerable interest to investigate the mechanism of action of (−)-MEP on AChE for the search of new MEP derivatives as AChE inhibitors.

Molecular docking is an efficient tool for investigating receptor-ligand interactions and for virtual screening, which plays a key role in rational drug design [13, 14],

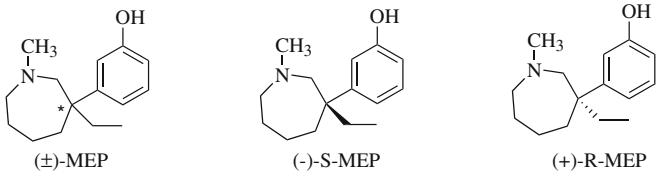

Fig. 1 The structures of (±)-MEP, (−)-MEP, and (+)-MEP

especially when the crystal structure of a receptor or enzyme is available. Almost all current docking programs, such as AutoDock [15], DOCK [16], FlexX [17], Glide [18] and GOLD [19], treat the ligand with full flexibility but assume the receptor to be rigid or apply very limited flexibility to side chains. Various searching algorithms such as fast shape matching (DOCK), simulated annealing (AutoDock), incremental construction (FlexX), genetic algorithms (GOLD), Monte Carlo (Ligand-Fit), and Tabu search, have been employed in docking studies [20]. Scoring functions are usually categorized as force-field based methods (such as DOCK and GOLD), empirical free-energy scoring functions (such as FlexX), and knowledge-based scoring functions [20] (such as PMF [21]). Among various docking algorithms, FlexX and GOLD are the two most reliable methods in complex validation tests [22].

Thusly, in the present study we first explored the feasibility of FlexX and GOLD on AChE with seven known AChE inhibitors whose complex structures with AChE [23] are available from the Protein Data Bank (PDB) [24], namely donepezil (E2020) [25], galanthamine (GNT) [26], BW284c51 [27], edrophonium (EDR) [28], huperzine A (HUPA) [29], huprine X (HUPX) [30], tacrine (THA) [31] (Fig. 2). The better of the two programs was then used as the docking protocol to investigate the binding mode of (−)-MEP on AChE. In addition, a small focused library with 91 bis-MEP derivatives (Fig. 3) was built and screened virtually using the specified docking method to give preferable candidates for synthesis. The compounds among the screening library included the bis-ligand derivatives of both enantiomers connected by spacers of length two to 14 carbons at substituents in N1- position (I) or C4- amino group (II) of the azepine ring. Bis-MEP derivatives were believed to make dual action, allowing interactions with both the ester-cleavage site and the peripheral anionic site (PAS) of AChE.

Materials and methods

The study was mainly performed on a R14000 SGI Fuel workstation. Molecular modeling and FlexX docking were carried out with the software package SYBYL version 6.9 [32]. The programs GOLD [33] and CORINA [34] were used for GOLD docking and 2 D to 3 D structural conversion, respectively. Standard parameters were used unless otherwise indicated.

Preparation of proteins

Three crystal structures of *Torpedo californica* AChE (*Tc*AChE) complexed with E2020 [25], HUPA [29] and THA [31] were retrieved from PDB [24] with corresponding entry code 1EVE, 1VOT and 1ACJ. The proteins were prepared by removing heteroatoms and water molecules and adding all hydrogen atoms. The active site of 1EVE was defined as residues with at least one atom within a radius of 10 Å from any atom of E2020. For 1VOT and 1ACJ, a 12 Å radius around the corresponding ligand was defined. The active sites were saved as PDB files for FlexX docking and MOL2 files for GOLD docking.

Preparation of known ligands for pose reproduction

The seven known AChE inhibitors were extracted from the corresponding complex structures with AChE, whose PDB codes are 1EVE, 1QTI, 1E3Q, 2ACK, 1VOT, 1E66, and 1ACJ, respectively. Atom types and bond types were

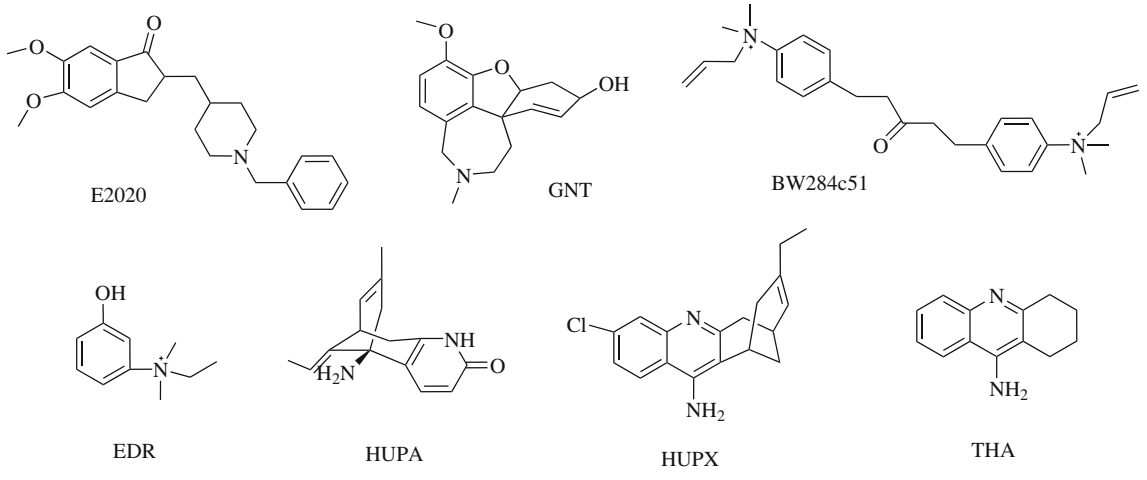

Fig. 2 Structures of seven known AChE inhibitors

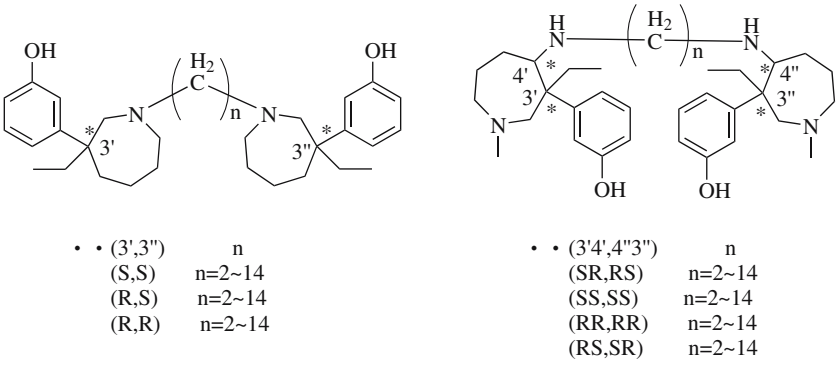

Fig. 3 Structures of designed bis-MEP derivatives

corrected manually. Hydrogen atoms and Gasteiger-Marsili [35] atomic charges were then added. The structures were minimized in SYBYL for 100 steps with the Tripos force field and saved to a multi-MOL2 file.

Preparation of focused library for virtual screening

Bis-MEP derivatives with spacer length of two to 14 carbons, a total of 91 molecules, were drawn in ISIS/Base with ISIS/Draw from MDL [36] and exported into a 2 D structure data file (SDF) to form a small focused library. The 2 D structures of the library were subsequently converted into 3 D-structures with CORINA [37], still in SDF format. The 3 D structures were then read into SYBYL Molecular SpreadSheet table for further treatment, such as energy minimization for 100 steps with Tripos force field and Gasteiger-Marsili [35] charges for each molecule. These structures were put into databases and then written to MOL2 files as input.

FlexX docking

All FlexX runs used the version 1.11.1 embedded within SYBYL. Formal charges were assigned and the FlexX scoring function was chosen to evaluate the docking poses.

GOLD docking

The default parameter settings for three times speed-up were used, and no flipping was allowed. In docking runs for pose reproduction, all ten solutions of each ligand were saved for further analysis. However, for virtual screening, only the best solution was kept for each molecule.

Results and discussion

Comparison of prediction accuracy of FlexX and GOLD

The accurate prediction of protein-ligand interaction geometries is essential for the success of virtual-screening approaches in structure-based drug design. It requires docking tools that are able to generate suitable conformations of a ligand within a protein binding site and reliable energetic evaluation indicating the quality of the interaction.

FlexX [17] uses an incremental construction algorithm where ligands are docked starting with a base fragment. The complete ligand is subsequently constructed by adding the remaining components. The best solution is selected according to the docking score, using a pure empirical scoring function by Böhm or a knowledge-based scoring function DrugScore. The GOLD [19] (Genetic Optimiza-

Table 1.a Fitness scores, RMSD from crystal structures and IC_{50} of known ligands by GOLD

		1EVE		1VOT		1ACJ		IC_{50} (nM)
	MOL_NAME	Fitness	RMSD (Å)	Fitness	RMSD (Å)	Fitness	RMSD (Å)	
Open	E2020	**66.15**	**0.5437**	48.64	3.3821	46.45	3.7311	**13.6**[a]
	GNT	**57.53**	**0.7819**	54.82	4.8748	53.29	4.2323	**1995**[a]
Half- open	BW284c51	80.28	3.5743	**85.36**	**4.1937**	63.42	3.6457	**0.0036**[b]
	EDR	44.09	4.2878	**43.93**	**1.2034**	46.02	4.1636	**240**[b]
	HUPA	46.35	3.6063	**50.78**	**1.2146**	51.55	0.528	**58.4**[a]
Closed	HUPX	59.94	5.3004	59.79	5.0281	**70.48**	**0.9428**	**0.026 (Ki)**[c]
	THA	45.13	5.8934	49.26	5.638	**50.47**	**5.6056**[d]	**93**[a]

[a]From Reference [47],
[b]From Reference [48],
[c]From Reference [49],
[d]Rank 2 scored 50.19 with an RMSD of 0.5404

Table 1.b. FlexX scores and RMSD from crystal structures and ligands by FlexX

MOL_NAME		1EVE		1VOT		1ACJ	
		F_Score	RMSD (Å)	F_Score	RMSD (Å)	F_Score	RMSD (Å)
Open	E2020	−12	17.545	−11.4	9.6344	−9.7	13.3023
	GNT	−27	0.5628	−11.3	15.4656	−24.7	0.7694
Half-Open	BW284c51	−8.9	7.049	−14.3	4.6601	−8.7	3.764
	EDR	−16.5	3.1461	−18	1.2315	−15.2	0.7693
	HUPA	−12.2	13.4537	−18.3	3.5703	−11.7	18.4646
Closed	HUPX	−14	16.688	−11.8	15.3927	−13.9	11.3687
	THA	−16.3	17.4666	−12.8	11.854	−13.5	14.7315

tion for Ligand Docking) program uses a genetic algorithm to explore the full range of ligand conformational flexibility and the rotational flexibility of selected receptor hydrogen atoms. The mechanism for ligand placement is based on fitting points, which are added to hydrogen-bonding or hydrophobic groups on both protein and ligand. And then the points between acceptors and donors map each other. The docking poses are ranked based on a molecular mechanics-like scoring function, named fitness function. These two protocols are verified as two of the most reliable methods in complex validation tests among various docking algorithms [22].

From a comparison of the published X-ray crystal structures of various *Tc*AChE complexes, it is obvious that the side-chain orientation of Phe330 is the only site with flexibility, which is responsible for substrate trafficking down the gorge. Three major orientations of Phe330 have been observed. The *Tc*AChE-E2020 complex (1EVE) is characterized by the open-gate conformation, while the complex with THA (1ACJ) displays a closed one, and the half-open conformation is observed in the *Tc*AChE-HUPA complex (1VOT) [38]. Since is still difficult to deal with flexibility of the protein thoroughly in current molecular docking methods, the open, half-open and closed gate conformations of AChE were investigated separately in this study to determine the importance of the side-chain flexibility of Phe330 for trafficking.

To explore the feasibility of the two methods FlexX and GOLD, we compared their predictive power of reproducing the binding poses of the known seven AChE complexes, namely the complexes of E2020 (1EVE) [25], GNT (1QTI) [26], BW284c51 (1E3Q), [27] EDR (2ACK), [28] HUPA (1VOT), [29] HUPX (1E66), [30] and THA (1ACJ) [31]. Among them, the first two complexes show open-gate conformations, whereas the last two form closed-gateway binding styles. And half-open gate structures are found for the middle three complexes. In the present study, we performed both FlexX and GOLD docking protocols on seven known AChE inhibitors. Taking three dominant orientations of the Phe330 side chain (open, half-open, and closed gate) into account, we have considered all three possibilities in separate docking runs for each of the seven ligands.

Scoring calculations showed that six of the seven ligands' optimal poses determined by GOLD were very close to the original orientation found in the crystal. The root mean square deviation (RMSD) for all heavy atoms between the docked and crystal ligand coordinates was below 1.5 Å with the exception of BW284c51, when the actual gate conformations of AChE were considered (highlighted in Table 1.a). And the fitness scores concluded from the actual gate conformations conformed to the inhibition activities as well (Table 1.a). The lower the IC_{50} of inhibitors was, the higher their fitness score showed. For the case of BW284c51, molecular complexity and flexibility might play a part in the failure of binding pose prediction. It is worth noting that FlexX performs better than GOLD in many cases. However, in the present exercise, it seemed that FlexX performed less well than GOLD (Table 1.b).

Table 2 Fitness score and evaluation of the interactions of (−)-MEP and (+)-MEP with TcAChE

Index		1EVE		1VOT		1ACJ	
		(−)-MEP	(+)-MEP	(−)-MEP	(+)-MEP	(−)-MEP	(+)-MEP
Fitness score		47.37	45.02	44.95	44.34	45.73	48.34
H-bond interactions	Donor	Ph-OH	–	Trp84-NH	Ph-OH, Ser122-OH	–	Ph-OH
	Acceptor	Glu199-O	None	Ph-O	Trp84-CO, Ph-O	None	Asp72-COO
	Distance/Å	1.953	–	2.557	2.681, 2.470	–	2.054
Hydrophobic interactions (distance/Å)	Ar[a]- Trp84	4.320	–	4.045	–	–	4.720
	Ar - Phe330	–	3.519	4.118	–	–	4.107
	Az[b]-Trp84	–	4.086	–	3.958	3.777	–
	Az - Phe330	4.003	–	–	–	4.281	–

[a]Ar—aromatic cycle of MEP
[b]Az—azepine cycle of MEP

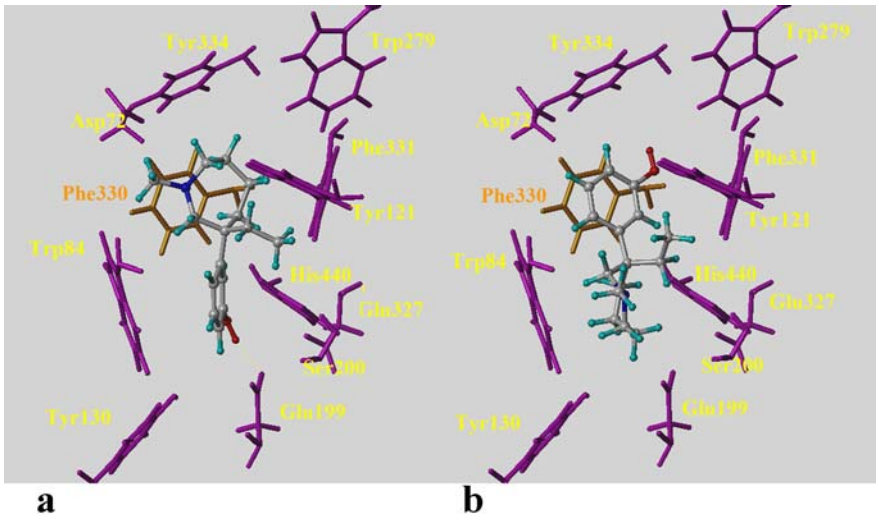

Fig. 4 Best docking solution of MEP into the open pocket (1EVE): **a** (−)-MEP (*left*); **b** (+)-MEP (*right*)

The low RMSD and the consistency of calculated affinity with experimental activity indicated that the GOLD method and parameter set were reasonable to reproduce the X-ray structure and could be extended to search and evaluate the binding poses of other AChE ligands accordingly.

On the other hand, comparison of the results of a specific ligand from three conformations of AChE demonstrated that the highest scoring pose was derived from the actual gate conformation and indicated the lowest RMSD. Thus, the experimental gate conformation of AChE complexed with an unknown ligand could be predicted roughly by comparing the fitness score concluded from three gate conformations of AChE.

Predicted binding conformation of (−)-MEP with AChE

The X-ray structure of AChE illustrated that the active site of the enzyme was a deep and narrow gorge with such features [39]: a catalytic triad composed of residues Ser200, Glu327 and His440; a peripheral anionic site at the entry centered by residue Trp279; and a hydrophobic site consisting of some aromatic residues such as Trp84 and Phe330.

In order to explore the mechanism of action of MEP isomers on AChE and explain the reason of their differences in activity, which is valuable for structure-based design of MEP derivatives with desired pharmacological properties, both *S* and *R* isomers of MEP were considered for GOLD docking runs. (−)-MEP and (+)-MEP were submitted to GOLD separately with the three gate conformations of AChE to consider the flexibility of the binding site of AChE.

Fitness scores of the best solutions and detailed interaction indices of both isomers are listed in Table 2. The hydrogen-bond (HB) interaction was evaluated by the distance between HB donor and acceptor atoms. The hydrophobic interaction was estimated according to the distance between the centroid of aromatic or azepine cycle of MEP and the centroid of the side train of the hydrophobic residue Trp84 or Phe330. Figs. 4, 5, 6 illustrated the binding maps of (−)-MEP and (+)-MEP with the binding site of three *Tc*AChE conformations.

The highest score of (−)-MEP was found for the open pocket (1EVE), while that of (+)-MEP was found for the closed one (1ACJ) (Table 2). Although the actual gate

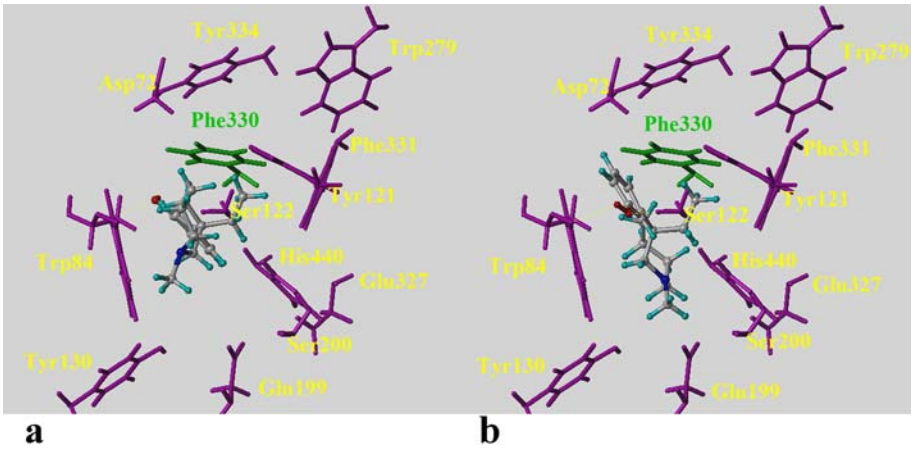

Fig. 5 Best docking solution of MEP into the half-open pocket (1VOT): **a** (−)-MEP (*left*); **b** (+)-MEP (*right*)

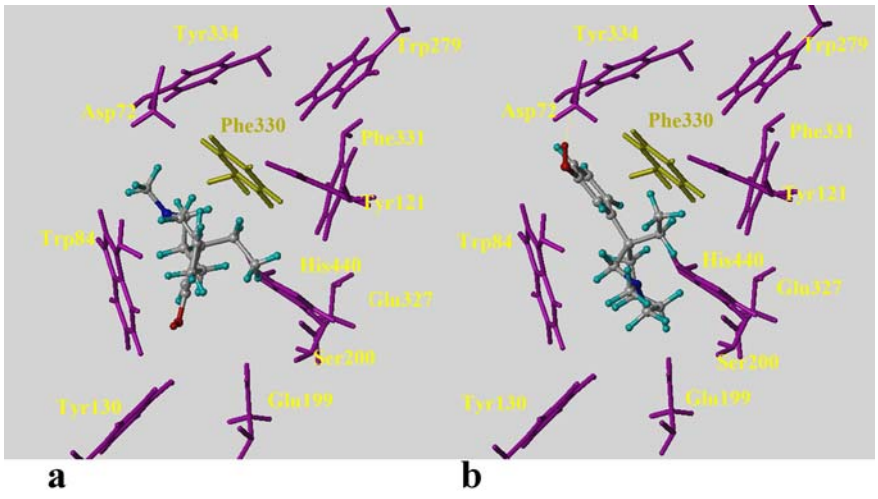

Fig. 6 Best docking solution of MEP into the closed pocket (1ACJ): **a** (−)-MEP (*left*); **b** (+)-MEP (*right*)

conformation of AChE binding with (−)-MEP and (+)-MEP might not be the same, their highest-score values did not conform to the activity data. In addition, up to now only rigid plane-shaped molecules like THA and HUPX were found bound in the closed gateway, forming a sandwich-like hydrophobic interaction. MEP, a flexible structure, did not seem to have enough chance of generating a closed-gate conformation (Fig. 6a and b).

The best-ranking poses of MEP isomers in the half-open pocket (1VOT) (Fig. 5a and b) adopted weaker and less specific HB interactions. The HB-forming distance was larger than those in other pockets. HB interactions with the amino or carbonylic group of the backbone of Trp84 were non-specific. Both the fitness score or the HB specificity and intensity suggest that 1VOT might not be the correct pocket for MEP.

As illuminated by Ennis' pharmacological experiments [11], (−)-MEP should score much higher than (+)-MEP, which was consistent with the scores derived from the open pocket. Therefore we thought that (−)-MEP and (+)-MEP both bound to the open-gate conformation of AChE similarly to the E2020-AChE complex (1EVE). In this binding site (Fig. 4a), the phenyl ring of (−)-MEP formed a face-to-face π-π stacking interaction with Trp84 (4.320 Å), and the seven-membered azepine ring of (−)-MEP formed a hydrophobic interaction with the side chain of Phe330 (4.003 Å). A strong HB, the absence of which caused the poor score of (+)-MEP (Fig. 4b), was formed between the hydroxyl of (−)-MEP and the carboxyl group of Glu199 (1.953 Å).

Results from virtual screening of bis-MEP by GOLD

In an effort to improve the potency and selectivity, the bivalent ligand strategy is applied to the development of new therapeutic agents. For AChE, drug units that have little or no intrinsic affinity can function as effective catalytic and/or peripheral site ligands when incorporated into a bivalent drug [40].

Based on the crystallographic structure of *Tc*AChE, two important active sites are involved: a catalytic triad located at the bottom of the cavity, and a PAS at the opening of the gorge. The distance between Trp 84 and Trp 279 is 12 Å [31]. We therefore presumed that the bis-ligands could interact simultaneously with the active and peripheral sites and thereby optimize the inhibiting potency. The potency of bis-THA [41, 42], bis-GNT [43], bis-HUPA [44], bis-HUPB [45], and bis-hupyridone, a simplified HUPA-like monomer [46], all significantly increased when linked by proper methylene spacers due to interactions with both the catalytic site and the PAS. Bis(7)-THA possessed both optimum AChE inhibition potency and AChE/butyrylcholinesterase (BChE) selectivity.

Aiming to find any molecules with high potency and selectivity for synthesis and further test, we designed 91 bis-MEP derivatives and screened them virtually on the basis of the methods established above. Two series of derivatives were classified based on the linkage position in the azepine cycle. Series I was linked at the N1-tertiary

Table 3 Rank, ID number, and the fitness scores of the top 15 bis-MEP derivatives

Rank	ID number	Seies number	*n*	Fitness score
1	bis_1_(*S*,*R*)_*n*=3	I (S,R)	3	69.19
2	bis_2_(*RS*,*SR*)_*n*=3	II (*RS*,*SR*)	3	68.17
3	bis_1_(*S*,*S*)_*n*=3	I (*S*,*S*)	3	63.85
4	bis_1_(*S*,*S*)_*n*=2	I (*S*,*S*)	2	62.24
5	bis_2_(*RS*,*SR*)_*n*=7	II (*RS*,*SR*)	7	61.52
6	bis_1_(*S*,*S*)_*n*=7	I (*S*,*S*)	7	61.12
7	bis_2_(*SR*,*RS*)_*n*=3	II (*SR*,*RS*)	3	60.76
8	bis_1_(*R*,*R*)_*n*=4	I (*R*,*R*)	4	57.56
9	bis_2_(*SR*,*RS*)_*n*=2	II (*SR*,*RS*)	2	56.51
10	bis_1_(*S*,*S*)_*n*=5	I (*S*,*S*)	5	55.5
11	bis_2_(*SR*,*RS*)_*n*=4	II (*SR*,*RS*)	4	55.47
12	bis_2_(*SR*,*RS*)_*n*=6	II (*SR*,*RS*)	6	55.35
13	bis_2_(*SR*,*RS*)_*n*=8	II (*SR*,*RS*)	8	55.27
14	bis_1_(*S*,*S*)_*n*=4	I (*S*,*S*)	4	55.1
15	bis_1_(*R*,*R*)_*n*=2	I (*R*,*R*)	2	55.08

amine position and Series II at the primary amine substituted position. Both enantiomers were combined successionally to consider the chiral influence of each monomer fully. Spacer lengths of the carbon bridge ranged from two to 14-carbons. The conformation of AChE was assumed to be open to allow the entrance of these bulky bis-ligands with long chain linkages.

Table 3 lists the chiral character, methylene group length, and fitness scores of the top 15 bis-MEP derivatives. Remarkably improved score values, the top two of which almost exceed that of E2020, suggested the potential optimization of potency. Interaction analysis (pictures omitted) showed that bis-MEP derivatives made good hydrophobic interactions with the residue Trp279 at the PAS. Comparing the chirality of the two series, we found that compounds derived from (−)-*S*-MEP with the *S*, *S*-conformation of Series I and the *SR*,*RS*-conformation of Series II dominated at the top of the list, which conformed with the activity of (−)-*S*-MEP versus (+)-*R*-MEP. Bis-MEP derivatives with a spacer of two to seven showed high score values, among which 3- and 7-methylene compounds were found to be the favored candidates. Under the guidance of these results, synthesis of the corresponding compounds is underway.

Conclusions

In this paper, we have established a useful docking method to predict the binding poses of AChE inhibitors. Using the GOLD docking protocol, the binding conformation and orientation of (−)-MEP with *Tc*AChE was illuminated and the potentially preferable bis-MEP derivative candidates were picked out by virtual screening. To our knowledge, this is the first exploration of the mechanism of action of MEP on AChE. Synthesis and biological evaluation of these selected analogues are currently underway and the results will be reported in the due course. Preliminary biological results implied that part of the candidates showed higher AChE inhibition than the core molecule (−)MEP. Although further biological results are needed to attest the actual predictive power of this method, the present study provides an alternate tool for structural optimization of (−)-MEP as new AChE inhibitors.

Acknowledgement We gratefully acknowledge financial support from the National Natural Science Foundation of China (Grant 30472088).

References

1. Marchbanks RM (1982) J Neurochem 39:9–15
2. Coyle JT, Price DL, Delong MR (1983) Science 219:1184–1190
3. Davis KL, Powchik P (1995) Lancet 345:625–630
4. Kawakami Y, Inoue A, Kawai T, Wakita M, Sugimoto H, Hopfinger AJ (1996) Bioorg Med Chem 4:1429–1446
5. Enz A, Boddeke H, Gray J, Spiegel R (1991) Ann NY Acad Sci 640:272–275
6. Greenblatt HM, Kryger G, Lewis T, Silman I, Sussman JL (1999) FEBS Lett 463:321–326
7. Zhang RW, Tang XC, Han YY, Sang GW, Zhang YD, Ma YX, Zhang CL, Yang RM (1991) Acta Pharmacol Sin 12:250–252
8. Ford JM, Truman CA, Wilcock GK, Roberts CJC (1993) Clin Pharmacol Ther 53:691–695
9. Hoskin PJ, Hanks GW (1991) Drugs 41:326–344
10. Bill DJ, Hartley JE, Stephens RJ, Thompson AM (1983) Br J Pharmacol 79:191–199
11. Ennis C, Haroun F, Lattimer N (1986) J Pharm Pharmacol 38:24–27
12. Chen Y (2004) Studies on the synthesis, resolution and optical isomers of meptazinol. Dissertation, Shanghai, Fudan University
13. Kuntz ID (1992) Science 257:1078–1082
14. Drews J (2000) Science 287:1960–1964
15. Morris GM, Goodsell DS, Halliday RS, Huey R, Hart WE, Belew RK, Olson AJ (1998) J Comput Chem 19:1639–1662
16. Kuntz ID, Blaney JM, Oatley SJ, Langidge R, Ferrin TE (1982) J Mol Biol 161:269–288
17. Rarey M, Kramer B, Lengauer T, Klebe GA (1996) J Mol Biol 261:470–489
18. Friesner RA, Banks JL, Murphy RB, Halgren TA, Klicic JJ, Mainz DT, Repasky MP, Knoll EH, Shelley M, Perry JK, Shaw DE, Francis P, Shenkin PS (2004) J Med Chem 47:1739–1749
19. Jones G, Willett P, Glen RC, Leach AR, Taylor R (1997) J Mol Biol 267:727–748
20. Hu X, Balaz S, Shelver WH (2004) J Mol Graph Model 22:293–307
21. Muegge I, Martin YC (1999) J Med Chem 42:791–804
22. Kontoyianni M, McClellan LM, Sokol GS (2004) J Med Chem 47:558–565
23. Greenblatt HM, Dvir H, Silman I, Sussman JL (2003) J Mol Neurosci 20:369–383
24. Berman HM, Westbrook J, Feng Z, Gilliland G, Bhat TN, Weissig H, Shindyalov IN, Bourne PE (2000) Nucleic Acids Res 28:235–242
25. Kryger G, Sliman I, Sussman JL (1999) Structure 7:297–307
26. Bartolucci C, Perola E, Pilger C, Fels G, Lamba D (2001) Proteins 42:182–191
27. Felder CE, Harel M, Silman I, Sussman JL (2002) Acta Crystallogr Sect D 58:1765–1771
28. Ravelli RBG, Raves ML, Ren Z, Bourgeois D, Roth M, Kroon J, Silman I, Sussman JL (1998) Acta Crystallogr Sect D 54:1359–1366
29. Raves ML, Harel M, Pang YP, Silman I, Kozikowski AP, Sussman JL (1997) Nat Struct Biol 4:57–63
30. Dvir H, Wong DM, Harel M, Barril X, Orozco M, Munoz-Torrero FJ, Luque D, Camps P, Rosenberry TL, Silman I, Sussman JL (2002) Biochemistry 41:2970–2981
31. Harel M, Schalk I, Ehret-Sabatier L, Bouet F, Goeldner M, Hirth C, Axelsen PH, Silman I, Sussman JL (1993) Proc Natl Acad Sci 90:9031–9035
32. SYBYL, version 6.9 (2002) Tripos Inc, St. Louis, MO, USA
33. GOLD, version 2.1. (2004) Cambridge Crystallographic Data Centre, Cambridge, UK
34. CORINA, version 3.0. (2004) Molecular Networks GmbH, Erlangen, Germany
35. Gasteiger J, Marsili M (1980) Tetrahedron 36:3219–3228
36. MDL 5.0 (2002) MDL Information Systems Inc, San Leandro, CA, USA
37. Gasteiger J, Rudolph C, Sadowski J (1990) Tetrahedron Comp Method 3:537–547
38. Pilger C, Bartolucci C, Lamba D, Tropsha A, Fels G (2001) J Mol Graph Model 19:288–296
39. Sussman JL, Harel M, Frolow F, Oefner C, Goldman A, Toker L, Silman I (1991) Science 253:872–879
40. Carlier PR, Chow ESH, Han YF, Jing Liu J, El Yazal J, Pang YP (1999) J Med Chem 42:4225–4231
41. Pang YP, Quiram P, Jelacic T, Hong F, Brimijoin S (1996) J Biol Chem 271:23646–23649

42. Carlier PR, Han YF, Chow ESH, Li CPL, Wang H, Lieu TX, Wong HS, Pang YP (1999) Bioorg Med Chem 7:351–357
43. Mary A, Renko DZ, Guillou C, Thal C (1998) Bioorg Med Chem 6:1835–1850
44. Wong DM, Greenblatt HM, Dvir H, Carlier PR, Han Y, Pang YP, Silman I, Sussman JL (2003) J Am Chem Soc 125:363–373
45. Xia Y (2002) The design and synthesis of Hup B derivatives based on the double active sites hypothesis of AchE. Dissertation, Shanghai, Shanghai Institute of Materia Medica Chinese Academy of Sciences
46. Carlier PR, Du DM, Han YF, Liu J, Perola E, Williams ID, Pang YP (2000) Angew Chem Int Ed 39:1775–1777
47. Tang XC (1996) Acta Pharmacol Sin 17:481–484
48. Frobert Y, Creminon C, Cousin X, Remy MH, Chatel JM, Bon S, Bon C, Grassi J (1997) Biochim Biophys Acta 1339:253–267
49. Camps P, Cusack B, Mallender WD, El Achab R, Morral J, Munoz-Torrero D, Rosenberry TL (2000) Mol Pharmacol 57:409–417